

1 A Superposition Model of Droplet and Aerosol
2 Risk in the Transmission of SARS-CoV-2

3 John E. McCarthy, PhD ¹
Washington University in St. Louis

4 Barry D. Dewitt, PhD ²
Department of Engineering & Public Policy
Carnegie Mellon University

5 Bob A. Dumas, PhD
Omnium LLC

6 James S. Bennett, PhD^{*}
Division of Field Studies and Engineering
National Institute for Occupational Safety and Health, CDC

7 KEYWORDS: covid-19, bioaerosols, droplets, airborne transmission, respiratory disease

8 Word count: 5,077

9 September 8, 2023

* Corresponding author email: jbennett@cdc.gov

Abstract

11 Considering three viral transmission routes – fomites, droplets, and aerosols
12 – two routes have been the focus of debate about the relative role of droplets
13 and aerosols in SARS-CoV-2 infection. We seek to quantify infection risk in
14 an enclosed space via short-range and long-range airborne transmission to
15 inform public health decision making. Data from five published studies were
16 analyzed to predict relative exposure at distances of 1m and farther, mediated
17 by droplet size divided into two bins: $\geq 8\mu\text{m}$ (medium and large droplets that
18 we call “droplets”) and $< 8\mu\text{m}$ (small droplets that we call “aerosols”). The
19 results at 1m from an infectious individual were treated as a boundary condi-
20 tion to model infection risk at shorter and longer distance. At all distances,
21 infection risk was treated as the sum of exposure to aerosols and droplets.
22 It was assumed that number of virions is proportional to particle volume.
23 The largest infection risk occurred close to the infectious individual, and
24 out to approximately 1m, droplets and aerosols both contributed. Farther
25 away, the largest risk was due to aerosols. For one model, droplet exposure
26 disappeared at 1.8m. Policy concerning physical distancing for meaningful
27 infection reduction relies on exposure as a function of distance, yet within
28 this construct particle size determines respiratory deposition. This two-fold
29 distance effect can be used to evaluate measures such as plexiglass barriers,
30 masking, and ventilation.

1 Introduction

There are believed to be three transmission routes for severe acute respiratory syndrome-coronavirus 2 (SARS-CoV-2): airborne transmission by droplets, airborne transmission by aerosols, and touching eyes, nose, or mouth with a hand that has touched an infected surface (fomite) or person [1]. The airborne routes have been the subject of debate and are clearly important[2], including the distinction between “droplets” and “aerosols” and their relative risk of causing infection [3, 4]. Fennelly [5] emphasizes the pathogen richness of droplets smaller than $5\text{ }\mu\text{m}$ in cough and exhalation plumes of persons with various respiratory infections, while acknowledging that SARS-CoV-2 is probably transmitted by “small and large particle aerosols.” Prather et al. [6] argue in a letter for a revision from the historical $5\text{ }\mu\text{m}$ divide between aerosols and droplets to a $100\text{ }\mu\text{m}$ threshold that better indicates where particle momentum dominates. In W. Chen (2020) [9] $100\text{ }\mu\text{m}$ is treated as the size where inhalation no longer dominates the short-range exposure. Dividing particles by size into either aerosols or droplets is confounded by the existence of three natural categories—sizes where particles closely follow the airflow; sizes where particles are influenced by the airflow, gravity, and their own momentum; and larger sizes where the effect of airflow is small. Using “aerosol” and “droplets” to denote behavior then corresponds to three behavior regimes: aerosol, aerosol and droplet, and droplet. In the current research, we divide particles into only two size ranges, aerosol ($< 8\mu\text{m}$) and droplets ($\geq 8\mu\text{m}$), with full recognition that defining droplets in this way includes inhalation exposure in much of this size range.

Many previous studies have modeled the complex dynamics of droplets launched from expulsive respiratory events, including host physiology and health state, as it affects droplet size, viscosity, number, and projection [7]. Long before the COVID-19 pandemic, the effects of cough-covering behavior were revealed in smoke visualizations and computational fluid dynamics (CFD), with [8] finding that covering with a tissue, a fist, or the elbow slowed horizontal momentum sufficiently for the droplets to move upward with the body’s thermal plume. A review by [9] of flow visualization techniques demonstrated interactions among the human respiratory and thermal plumes and space airflows in hospital settings. Notably, a Schlieren image showed that a surgical mask stopped the turbulent cough jet from penetrating forward into room air but diverted it upward into the thermal plume. Ai and Melikov [10] reviewed approximately 200 studies and concluded that

boundary conditions, simplifying assumptions, and insufficient time resolution have led to inconsistencies, which require further work in understanding indoor airflow patterns. Added to the variability due to initial conditions and indoor airflows are the many effects of the size of evaporating droplets on trajectory, intake, and viral load [11]. Although most droplets in their model were $8-16\mu\text{m}$, they concluded $32-40\mu\text{m}$ could lead to more infections due to higher viral content. Humidity and temperature affecting droplet size and virus viability was considered in [12], [13], [14], [15], and [16].

A spatially detailed CFD analysis that includes many factors in a simulation of a conversation across a dining table, notably masks and N95 respirators, is reported by [17]. Particle image velocimetry (PIV) validated their simulation. The near field, defined here as within 1m of a respiratory source, has received intense research interest, with measurements often occurring only at 1m. Coldrick et al. [18] extended the range to compare findings at 1m and 2m. CFD models tracked droplets in the warm, humid plume, and experiments assayed bacteria in respiratory and oral droplets generated by human subjects coughing, speaking, and singing. Each approach showed greater deposition of bacteria within 1m and, for droplets smaller than $10\mu\text{m}$, no clear difference in airborne concentrations at 1m and 2m. The zone of 0.2 to 2m from the subject was analyzed in a CFD study by [19] that connected two strong themes in COVID-19 research: the importance of the inhalation route of exposure and greater infection risk at close distances.

Distance between a potential infector and a susceptible is clearly important, but distance is a sort of summary variable which contains (and possibly obscures) the time-dynamic biological, chemical, and physical processes occurring as an infectious plume moves outward. Measurement at a specific distance is a snapshot in time when these processes have progressed to an extent toward their resolution. Deconstructing the overall “distance effect” into particle size and exposure route, though difficult, can help to clarify the many terms that have been used throughout the pandemic, such as “close contact” and “aerosol.” In the current study that analyzes published data and models, we combine results at various distances to arrive at some examples of infection risk distance functions. The obvious uncertainty in each piece of such a model constrains the present work to simply be an illustration of placing specific results in a quantitative gestalt.

Although it is now clearer to the broader research community and the public that the threshold between “droplet” and “aerosol” is dynamic [3], depending on both the pathogen and environmental conditions, the relative

106 importance of droplets and aerosols to infection risks, and the consequences
 107 for mitigation policies, is not a settled matter. A report from the UK’s
 108 Scientific Advisory Group for Emergencies estimated the risk of SARS-CoV-2
 109 infection for a non-infected person standing at 1m from an infectious person
 110 to be at most an order of magnitude larger than the risk of infection at
 111 double that distance [20]. We endeavor to improve on estimates of that kind,
 112 by comparing the relative viral loads received through standing close to an
 113 infectious person with the amount received more generally indoors, such as
 114 in classrooms, airplanes, and stadiums. We leverage results from previous
 115 empirical research to better model infection risk, potentially as input to risk-
 116 cost-benefit analyses of common activities for public and private decision-
 117 making [21].

118 Given that most existing buildings were constructed during decades when
 119 the idea of using ventilation to prevent infectious disease was out of favor
 120 [22], many built environments can be loci of SARS-COV-2 spread. Here, we
 121 attempt to estimate the risks of aerial transmission, operationalized as the
 122 quantity of virus in particles exhaled by an infected person and inhaled by
 123 a currently uninfected person. We first describe our terminology and the
 124 conceptual model. We then incorporate data from the literature to estimate
 125 viral loads due to aerial transmission and include estimates derived from bac-
 126 teriophage droplet tracer studies, for possible exposure during a commercial
 127 flight. Finally, we discuss implications for policymaking.

128 **2 Methods**

129 **2.1 Droplets and Virions**

130 Our conceptual model is the following: when an infected person exhales (or
 131 vocalizes, coughs or sneezes) they spray a plume of droplets and aerosols
 132 that contain the virus into the air. The droplets may collide with a person
 133 (including landing on the nose or in the mouth or eyes), be inhaled, land on
 134 a surface, or fall to the ground. The aerosols can waft through the air for
 135 minutes or hours (depending on the air change rate), travel a long distance,
 136 and potentially reach a distant person, where inhalation is the most likely
 137 exposure route. We estimate the number of virions dispersed via the respira-
 138 tory tract of an infected person to be proportional to the initial droplet size
 139 as volume. Then, we compare those quantities at different distances to get

140 a better estimate of the exposure by making a chain of inferences explained
141 at length below.

142 2.2 Data

143 The terms “droplet” and “aerosol” are often used in the literature with re-
144 spect to whether they pose *short-range* or *long-range* airborne transmission
145 risk. It is desirable to not require a constant size threshold to separate the
146 particles defined by the two terms, which is a common, but much-criticized,
147 practice [3]. In this study, we do apply a size threshold to align with cited
148 literature that separates droplets into small and medium/large bins.

149 In Subsection 2.4 we use theoretical results of Chen et al. [23] to estimate
150 the short-range risk from emitted droplets and aerosol. In Subsection 2.5 we
151 use experimental results of Shah et al. [24] to estimate the long-range risk
152 from aerosols for a given rate of aerosol emission. We then use experimental
153 results of Duguid [25] and Chao et al. [26] to estimate what fraction of
154 exhaled particles contributes to risk as aerosols and what fraction contributes
155 as droplets. Subsection 3.1 compares the risk at distances 1m versus 2m.

156 2.3 Alice and Bob: a Scenario

157 To provide definitions, list assumptions, and outline the analytical procedure
158 (Figure 1), we use the following scenario: An infectious individual, whom we
159 shall call Alice, poses an airborne infection risk to a non-infected individual,
160 whom we shall call Bob. We proceed as follows:

- 161 1. Bob is in an enclosed environment with Alice for an extended period of
162 time (an hour or more). Alice is exhaling saliva and lung fluid droplets
163 of different sizes, all with the same expected concentration of virions
164 per unit volume, initially, at launch. We classify Alice’s droplets into
165 two bins by size.
- 166 2. For the purpose of this model, droplets with diameter $\geq 8\mu\text{m}$ we call
167 *droplets*. These are pulled down by gravity, but slowly for smaller sizes
168 in this range. Using [27] and [28], Maynard [29] reports that a $58.5\mu\text{m}$
169 particle falls 1m in 10s, in still air. Droplets pose risk to Bob if they
170 land in his mouth, nose or eyes as projectiles. We call this transmission
171 route *Route 1*. They may also be inhaled, and we call this transmission
172 route *Route 2*.

- 173 3. Droplets with diameter $< 8\mu\text{m}$ we call *aerosols*. These drift in the air,
174 where a $7.4\mu\text{m}$ particle will drop 1m in 10 min. [Maynard 2020]. The
175 risk they pose to Bob is mainly if he inhales them (Route 2).
- 176 4. In Table 1, we give measurements from [26] and [25] of the ratio of
177 volumes for total exhalation in droplets to total exhalation in aerosol.
178 We call this ratio ρ . The fraction of the total emission of all particles
179 that is aerosol is then $\frac{1}{\rho+1}$.
- 180 5. From [23], we get that every $1\mu\text{L}$ of exhaled droplets produces 17×10^{-6}
181 μL of exposure via Route 1 and Route 2 if Bob is facing Alice at a
182 distance of 1m. At this distance the short-range airborne subroute of
183 Chen et al. (our Routes 1 and 2) dominates their large droplet subroute.
- 184 6. To extrapolate what the short-range airborne exposure would be at
185 different distances, we use two models: a rapid decay model from [23]
186 and an inverse distance square decrease.
- 187 7. For the Route 2 exposure, we use the experimental data of [24]. That
188 study measures what fraction of a given aerosol emission is inhaled at a
189 distance of 2m. We multiply this fraction by $\frac{1}{\rho+1}$ to estimate the total
190 inhalation of aerosols by Bob via Route 2 at a distance of 2m for every
191 $1\mu\text{L}$ of droplets exhaled by Alice.
- 192 8. To extrapolate the aerosol inhalation (Route 2) at different distances,
193 we use the bacteriophage measurements in Boeing 737 and 767 aircraft
194 cabin mock-ups of [30].
- 195 9. The total exposure of Bob is the sum of the Route 1 and Route 2
196 exposures. We assume that Bob's risk of infection is proportional to
197 the total exposure.

	Chao Speak	Chao Cough	Duguid Speak	Duguid Cough	Duguid Sneeze
Vol. (μL) in Aerosol	3E-06	6E-06	6E-06	1E-04	4E-02
Vol. (μL) in Droplets	8E-04	1E-03	5E-03	9E-02	9
Ratio (Droplets/Aerosol)	270	160	760	786	200

Table 1: Volume of various droplet sizes from Chao (2009) [26] (C) and Duguid (1946) [25] (D).

198 Using the setup described above, we estimate the risks posed by Route 1
 199 and Route 2 exposure in the setting of commercial passenger aircraft.

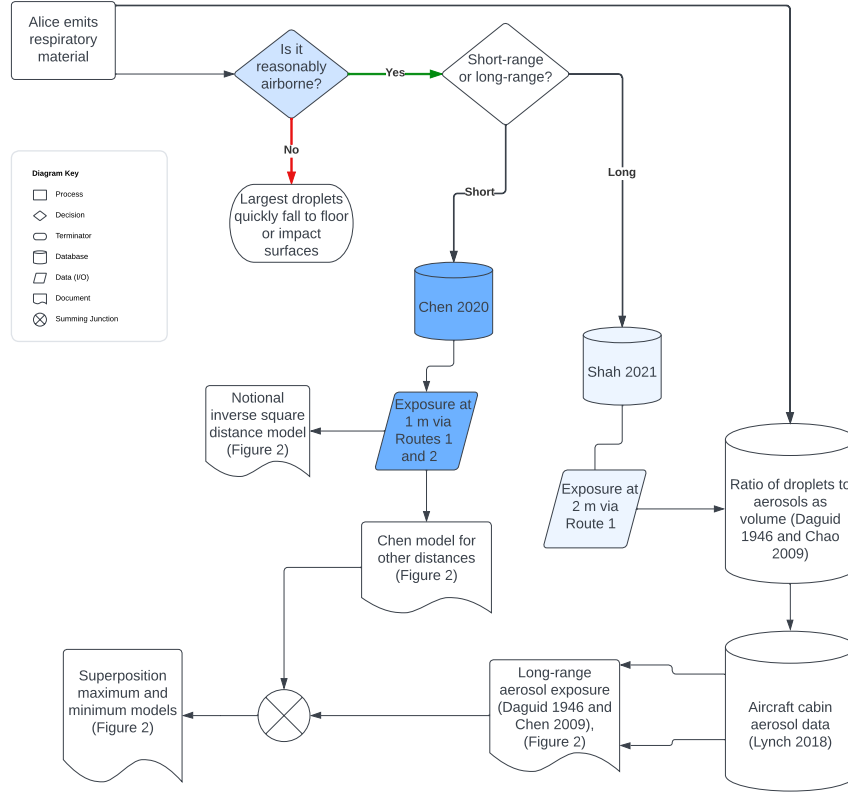


Figure 1: Flowchart illustrating how five published studies (Chen 2020 [23], Duguid 1946 [25], Chao 2009 [26], Shah 2021 [24], Lynch 2018 [30]) are used to form the current model involving distance, particle size (droplets, aerosol) and exposure route (Routes 1 & 2).

200 2.4 Droplet exposure: Routes 1 and 2

201 In [23], Chen et al. analyze short-range transmission based on a data-driven
 202 mathematical model. They assert two main routes of short-range non-fomite
 203 transmission: particles that are projected directly into the mouth, nose and

eyes of a nearby facing person at the same height (they ignore droplets that hit any other part of the face or body) and particles that follow the air stream and are inhaled. Large droplets are intrinsically short-range, because gravity pulls them down to the floor in a short period of time (However, if coughed out, they can travel a long distance horizontally.). They conclude that mid-size droplets (defined as having initial diameters of $75 - 400\mu\text{m}$) travel the shortest distance, because they can fall to the ground somewhat rapidly—within 1m (talking) and 2m (coughing), but are too large for airflow carriage over distance and too small for long range ballistic projection. Smaller droplets follow the airflow and travel farther; larger ones have more inertia, so will also travel farther, but will settle to the ground unless they impact another surface. Moreover, they conclude that at distances over 0.3m (talking) and over 0.8m (coughing) the majority of exposure comes from inhaled droplets rather than deposited droplets.

For their base data, [23] use a paper by Duguid [25] that measured the number and size of droplets exhaled by a person coughing, and by counting loudly from 1 to 100. The latter produced a total measured volume of $0.36\mu\text{L}$ (of which $2 \times 10^{-3} \mu\text{L}$ came from droplets with a diameter less than $75\mu\text{m}$). The conclusion of [23] that we will use with respect to short-range airborne transmission is that face-to-face, at a range of 1m, a person inhales $6.2 \times 10^{-6} \mu\text{L}$ of the original $0.36 \mu\text{L}$ of the talking emission, almost all of it from droplets smaller than $75 \mu\text{m}$. Dividing by 0.36 we get that every 1 μL of exhaled droplets produces 17pL of inhaled droplets, via Route 1, from a facing subject at 1m (we change from μL to pL to make the numbers easier to read and compare).

We shall then multiply the number 17pL by a function depending on distance from the source to get the exposure at different distances. We shall refer to this technique of estimating the exposure at a specific distance and then multiplying by a function that decreases with distance as anchoring. The short-range distance functions decay more rapidly than the long-range ones.

2.5 Route 2: Aerosol exposure

In [24], Shah et al. set up a mannikin with a mechanical ventilator that exhaled atomized olive oil droplets, with a mean diameter of $1 \mu\text{m}$. The concentration c of oil in the air was measured for ten hours at a distance of 2 m. Olive oil was chosen because its use with the experimental setup produced

240 particles of similar sizes to those produced during human exhalation. They
 241 fit their results to the following single-box mass balance model:

$$\frac{dc}{dt} = R - \lambda c, \quad (1)$$

242 where c is the time-dependent concentration in *particles/m³*, R is the particle
 243 injection rate R in *particles/m³s*, and λ is the particle decay rate in s^{-1} .

244 Equation (1) simplifies the time-dependent diffusion equation (including
 245 sources, R , and sinks, λc), by assuming instantaneous uniform distribution
 246 of the aerosols. Operationally, this simplification was made by removing the
 247 diffusion term, $\nabla \cdot K \nabla c$, where K is the diffusion coefficient in m^2/s . Its
 248 solution, assuming the initial concentration is zero, is given by

$$c^*(t) = \frac{R^*}{\lambda^*} (1 - e^{-\lambda^* t}). \quad (2)$$

249 Shah's asterisk notation in Equation (2) is to acknowledge that the injec-
 250 tion rate and decay rate in this solution are accounting for some diffusion
 251 effects, since there is no explicit diffusion term. The asterisked concentration
 252 represents the specific measurement location 2 m from the source, so that
 253 Equation 1 need only hold there, rather than throughout the whole space.
 254 While the particle source is active, the quantity $c^*(t)$ from Equation (2) will
 255 tend asymptotically to $c_{\text{sat}}^* = \frac{R^*}{\lambda^*}$.

256 Shah et al. [24] measured the concentration of particles at a 2-meter
 257 distance from the mannikin, with and without a mask on the source man-
 258 nikin and at different ventilation rates, indicated as air changes per hour
 259 (ACH). Table 2 summarizes some of their results for several masking and
 260 ACH combinations.

Mask	ACH	R^* (% h^{-1})	λ^* (h^{-1})	$c_{\text{sat}}^* = R^*/\lambda^*$
None	0	0.53 ± 0.11	0.46 ± 0.11	1.13 ± 0.057
Surgical**	0	0.41 ± 0.36	0.41 ± 0.39	0.99 ± 0.11
None	1.7	0.48	1.36	0.35
None	3.2	0.41	2.27	0.18

**Source masking only

Table 2: Adapted from Shah (2021) [24]. First column indicates whether the exhaling mannikin is wearing a mask. Second column is the number of air changes per hour. Third column is the percentage of exhaled particles that arrive at the detector every hour. Fourth column is the particle loss rate parameter. Fifth column is the steady state or saturation concentration as a percentage of the emission rate.

Thus, for example, at a distance of 2m, they found that the concentration was 1.13% (± 0.057 %) of the breath particle injection rate (final column, second row of Table 2). Note that even though the surgical mask material was measured to be 47% effective at blocking particles flowing through it, an amount visible through laser-sheet illumination escaped upward around the bridge of the nose, thus diminishing its effectiveness when worn.

Using the values of R^* and λ^* from Table 2 and equation 2, we get the estimate at 2m of

$$c^*(t) = 0.0113R(1 - e^{-0.46t}). \quad (3)$$

Equation 3 has little directional dependence: Shah et al. did measure at a distance of 2m and at angles of 0° , 90° and 180° from the source, and found the variation to be less than 10%.

3 Results

3.1 Comparing Route 1 and Route 2 exposures

Table 3 shows the aerosol exposure at 2m for a given emission rate. From [23], we get that every 1 μL of exhaled droplets produces 17pL of inhaled droplets from a facing subject at 1m. We estimate the long-range risk by first using the values from Table 1 to estimate the fraction of that 1 μL that is aerosolized, and then use the data from Table 2 to estimate how much of that is inhaled at steady state conditions at a distance of 2m. We assume an exhaled particle is aerosolized when it has a diameter $\geq 8 \mu m$,

281 although environmental conditions change the diameter at which particles
 282 remain airborne [3].

283 These assumptions yield the following table. The columns use the mea-
 284 surements from Chao (2009) [26] and Duguid (1946) [25]. The rows are the
 285 four conditions in Table 2.

Mask	ACH	Chao Speak	Chao Cough	Duguid Speak	Duguid Cough	Duguid Sneeze
No	0	41	68	14	14	55
Surgical**	0	37	61	13	13	49
No	1.7	13	22	4.6	4.5	17
No	3.2	6.7	11	2.4	2.3	9

**Source masking only

Table 3: Steady-state aerosol intake in pL for every $1 \mu L$ emitted, at a 2m distance from the source (from Chao (2009) [26], Duguid (1946) [25], and Shah (2021) [24]).

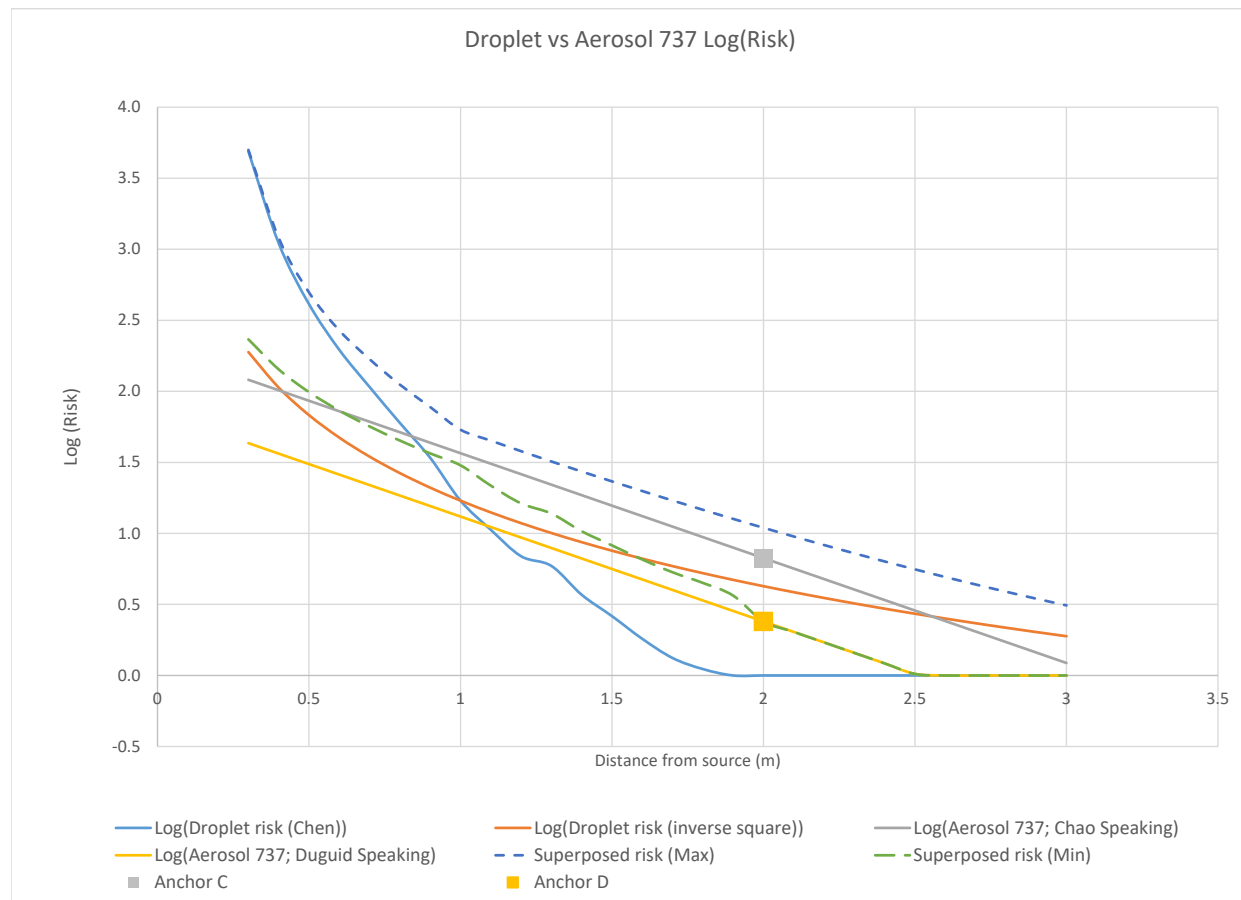
286 The first entry, for example, is taken by dividing $1 \mu L$ by 271, which
 287 Table 1 tells us is the fraction of the original emission that is aerosolized
 288 using the measurements from [26] and the assumption that only the small
 289 droplets become aerosolized, and then multiplying this number by 1.13%
 290 which comes from the last column in Table 2.

291 3.2 Decay with distance

292 As far as we are aware, no one is certain how the risk from either droplets or
 293 aerosols decays with distance from the source. For droplets, the theoretical
 294 model of [23] has a very rapid decay with distance. To compare it with a
 295 more conservative estimate, we also model the decay as inverse square with
 296 distance. We shall anchor the latter with the same exposure at 1m from the
 297 Chen et al. model.

298 For aerosols, the Lynch study [30] of aerosol decay with distance in air-
 299 craft cabins reported that their best fit for a single-aisle Boeing 737 was
 300 $e^{-1.7x}$, where x is the distance from the source in meters, and for a twin-aisle
 301 Boeing 767 it was $e^{-.47x}$. Anchoring with the measurement from Table 3 with
 302 the largest measured ventilation, 3.2 ACH, the resulting aircraft cabin expo-
 303 nential decay curves plotted on the log scale are the straight lines in Figure
 304 2. The air change rate of the cabins is approximately 32 ACH, ten times

305 higher than Shah's highest rate, meaning that the rate of aerosol removal
 306 was about three times faster. However, the magnitude of these long-range
 307 curves (where they are on the vertical axis) is set by the Shah data. In the
 308 absence of mechanical ventilation, the decrease of aerosol risk with distance
 309 is likely to depend on thermal plumes of occupants and natural infiltration.



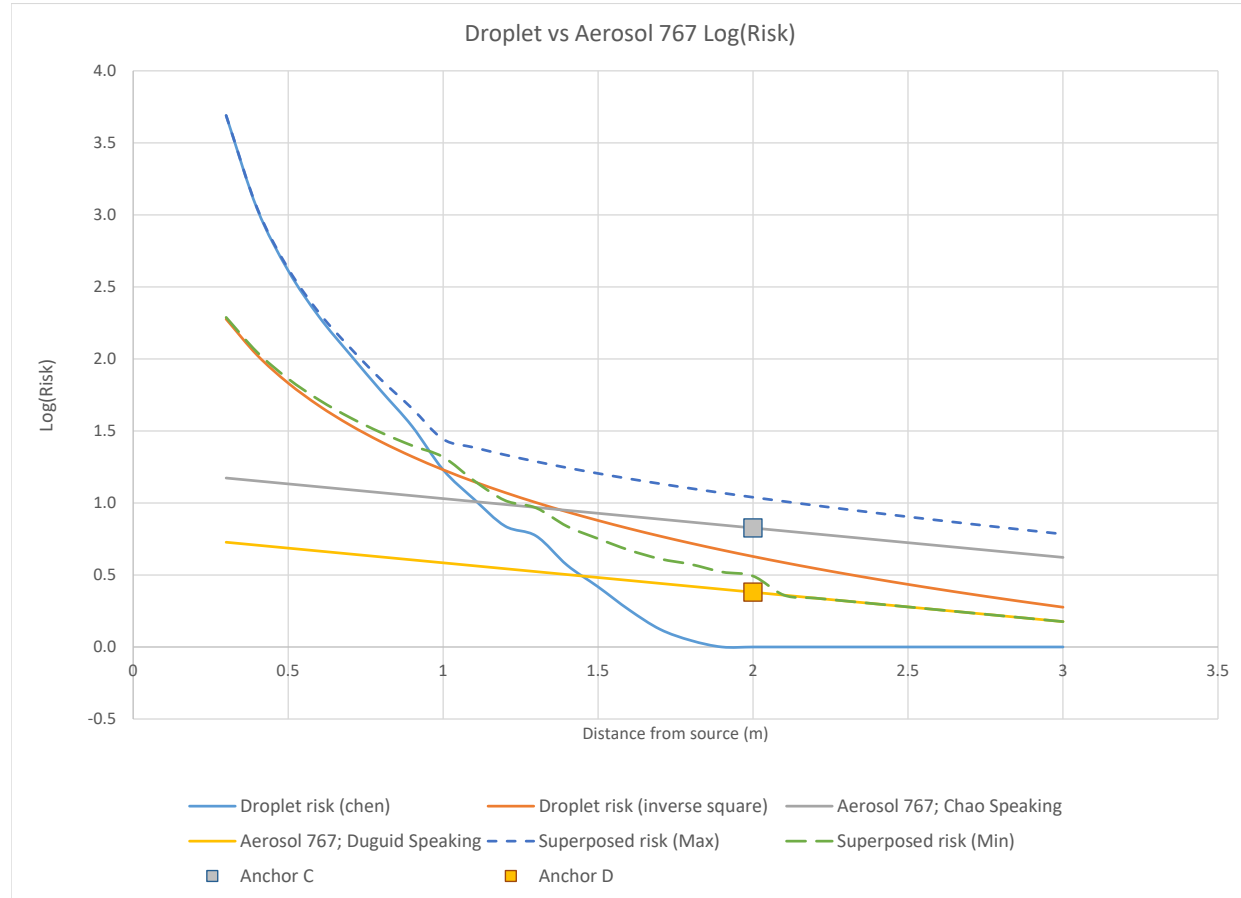


Figure 2: Decrease of risk, as virion exposure, with distance from an infectious person. The key finding is that for short distances both Routes 1 and 2 are important sources of exposure (estimated in two different ways, shown by blue and orange curves), because the decay is steeper than for the long-range models. For these longer distances the primary source of exposure is aerosols and Route 2 (estimated in two different ways, shown by gray and yellow curves). The decrease measured in 737 (first Figure) and 767 (second Figure) mock-up tracer experiments is normalized or “anchored” to intersect the speaking data at 2m from Chao (gray) and Duguid (yellow). The anchor values from Table 3 are plotted on the log base 10 scale. The superposed risk is the sum of the droplet and aerosol exposure risk. We plot the sum of the maximum and the minimum of the two estimates and note that these are larger than the trend predicted by the long-range data.

310 4 Discussion

311 Figure 2 shows that selection of effective interventions to reduce exposure
312 must consider how the short- and long-range routes differ. Even these rough
313 estimates based on these models show the relative magnitudes of droplets and
314 aerosol exposures as a function of distance. Starting closest to the source,
315 the very steep descent of Chen’s model (light blue) indicates the presence
316 of droplets, including large ones that fall to the ground within 1 m, unless
317 their launch velocity carries them far as projectiles. This curve slopes down-
318 ward faster than an inverse square function (orange). More gradual still are
319 the exponential drops of the aircraft cabin curves (straight lines in the log
320 plot). Short-range exposures include direct contact (Route 1) and inhalation
321 (Route 2). Long-range exposures shown by the cabin data represent Route 2.
322 The fact that these distance reduction curves differ greatly suggests Route 2
323 cannot account by itself for the short-range risk. Therefore, Route 1 must be
324 important. Interventions that mitigate Route 1, such as plexiglass barriers
325 between a customer and a store cashier would then have efficacy; in contrast,
326 Route 2 dominating farther away shows how ventilation, filtration, and air
327 disinfection would be paramount. Of course, interventions such as respira-
328 tors or masks (worn by both infectious and susceptible) can reduce the risk
329 from both routes.

330 The superposed exposure curves (dark blue and green) further indicate
331 the importance of Route 1, as these lines are closer to the short-range than
332 they are to the long-range lines. They actually converge to the short-range
333 lines as source distance decreases. The situation is that adding the exposure
334 from Route 2 to the combined exposures from both Routes 1 and 2 makes
335 little difference when within 1 m of the source. One interpretation of this
336 outcome is that direct contact by droplets dominates the total exposure in
337 this short range.

338 By combining the results from previous empirical and modeling research
339 [26, 23, 25, 30, 24], this study has produced a simple model that aggregates
340 the short-range (i.e., droplet and aerosol) and long-range (i.e., aerosol) air-
341 borne risks to produce estimates of virion intake. In Lynch (2018) [12], the
342 aircraft cabin results were generated by visible droplet spray of bacteriophage
343 solution that evaporated to droplet nuclei in the mock-up cabin environ-
344 ment before measurement at distances of 0.5 to 8m. While that generation
345 method produced droplets and aerosol at the source, the measurement dis-
346 tances probably favored aerosol over droplets, certainly over large droplets.

347 Aircraft cabins and other environments would be better characterized by
348 more measurements close to infection sources, so that this critical zone could
349 be understood in more detail than what is provided by whole-space decay
350 models. The present study is limited by synthesizing results from multiple
351 studies using different methods, and could be improved by data that were all
352 collected using the same experimental procedures.

353 The estimates of superposed risk from Figure 2 should be compared with
354 Figure 1b in [31], which provides a power law fit to distance for the spatial
355 distribution of droplet mass in an aircraft cabin reported in Zee et al. [32].
356 Their work modeled a cough source, including evaporation in low humidity
357 cabin air, using computational fluid dynamics.

358 Our assumption that infection risk is proportional to droplet volume is a
359 limitation. As droplets evaporate and shrink toward their nucleus of possi-
360 bly infectious material, the number and viability of virions may or may not
361 change. The long-range data from droplet spray in Lynch (2018) [30] con-
362 sisted mainly of evaporated droplet nuclei, based on the average residence
363 time being longer than the evaporation time. Pease et al. [12] investigated
364 some mechanisms for enveloped viruses such as SARS-CoV-2 to maintain
365 or lose viability. A related weakness is that we relate infection risk directly
366 to exposure taken in, without regard to interactions with tissue, infection
367 thresholds, and individual susceptibility.

368 All of the estimates presented here highlight the importance of mask use
369 by all persons, which lowers the risks to those close to an infected person
370 [33] and at greater distances. Estimates of virion intake depended on the
371 model used (Figure 2); and, given uncertainties in viral-shedding and in how
372 infection risk scales with exposure duration [34], the use of **measures such as**
373 **masks, vaccination, and testing**, for persons who choose to participate in
374 optional activities near others is justifiable. When the infectivity of nearby
375 occupants is unknown and unchangeable, such as on commercial airplanes or
376 at sporting events with full seating, perhaps no personally-chosen mitigation
377 is available beyond wearing a high-quality mask. Fundamentally, Figure 2
378 show that physical distancing reduces exposure from both short- and long-
379 range routes and should be considered as an administrative control layer
380 within the prevention strategy.

5 Conclusion

The importance of droplets and aerosol in SARS-CoV-2 infection has been the focus of debate, and we have provided some quantification of the relative roles of these size ranges. Using five published studies, we have developed a model that suggests the largest infection risk (as exposure to droplet volume) came from droplets (particles of $8\mu\text{m}$ and larger), when close to the infectious individual out to approximately 1m. Farther away, the largest risk was due to aerosols (particles smaller than $8\mu\text{m}$). Because the risk exposure by particle size has been estimated in different ways, and moreover depends on varying environmental and spatial characteristics, we cannot say exactly at what distance aerosol and associated mechanisms become the primary source of exposure, but it seems to be approximately 1m.

That droplets are important close to a source comes as no surprise, when droplet inhalation is recognized as an exposure route that contributes along with direct contact to short-range risk, but verification of this intuition is a step toward focusing public health measures. These trends emerged while summing the contributions of both size ranges to estimate the total exposure. Policy concerning physical distancing for meaningful infection reduction relies on exposure as a function of distance, yet within this construct particle size determines respiratory deposition. This two-fold distance effect can be used to evaluate additional measures such as plexiglass barriers, masking, and ventilation. Duguid’s observation in 1946 about collecting respiratory droplets on glass slides is relevant today, for the uses and limitations of barriers: “Few droplets were found of less than $10\mu\text{m}$ in diameter and none of less than $5\mu\text{m}$. It is presumed that droplets smaller than this possessed such a small mass, or evaporated rapidly to such a small mass, that they were carried past the slide in the deflected air stream.”

Disclosures. The authors have no conflicts of interest relevant to this article. McCarthy was partially supported by National Science Foundation Grant DMS 2054199. Dewitt was supported by the Riksbankens Jubileumsfond (Swedish Foundation for the Social Sciences and Humanities) program on Science and Proven Experience.

References

- [1] CDC. How COVID-19 Spreads. <https://www.cdc.gov/coronavirus/2019-ncov/prevent-getting-sick/how-covid-spreads.html>, 2021.
- [2] Trisha Greenhalgh, Jose L. Jimenez, Kimberly A. Prather, Zeynep Tufekci, David Fisman, and Robert Schooley. Ten scientific reasons in support of airborne transmission of SARS-CoV-2. *The Lancet*, 397(10285):1603–1605, 2021.

- 415 [3] K Randall, E T Ewing, Linsey C Marr, J L Jimenez, and L Bourouiba.
416 How did we get here: what are droplets and aerosols and how far do
417 they go? A historical perspective on the transmission of respiratory
418 infectious diseases. Interface Focus, 11(6):1–17, dec 2021.
- 419 [4] Prateek Bahl, Con Doolan, Charitha de Silva, Abrar Ahmad Chughtai,
420 Lydia Bourouiba, and C Raina MacIntyre. Airborne or Droplet Pre-
421 cautions for Health Workers Treating Coronavirus Disease 2019? The
422 Journal of Infectious Diseases, pages 1–8, 2020.
- 423 [5] Kevin P Fennelly. Particle sizes of infectious aerosols: implications for
424 infection control. The Lancet Respiratory Medicine, 8(9):914–924, 2020.
- 425 [6] Kimberly A. Prather, Linsey C. Marr, Robert T. Schooley, Melissa A.
426 McDiarmid, Mary E. Wilson, and Donald K. Milton. Airborne trans-
427 mission of sars-cov-2. Science, 370(6514):303–304, 2020.
- 428 [7] D. Fontes, J. Reyes, K. Ahmed, and M. Kinzel. A study of fluid dynamics
429 and human physiology factors driving droplet dispersion from a human
430 sneeze. Physics of Fluids, 32(11), 11 2020. 111904.
- 431 [8] C. Chen, C.-H. Lin, Z. Jiang, and Q. Chen. Simplified models for exhaled
432 airflow from a cough with the mouth covered. Indoor Air, 24(6):580–591,
433 2014.
- 434 [9] J.W. Tang, C.J. Noakes, P.V. Nielsen, I. Eames, A. Nicolle, Y. Li, and
435 G.S. Settles. Observing and quantifying airflows in the infection con-
436 trol of aerosol- and airborne-transmitted diseases: an overview of ap-
437 proaches. Journal of Hospital Infection, 77(3):213–222, 2011. Proceed-
438 ings from the Sporicidal Workshop.
- 439 [10] Z. T. Ai and A. K. Melikov. Airborne spread of expiratory droplet nuclei
440 between the occupants of indoor environments: A review. Indoor Air,
441 28(4):500–524, 2018.
- 442 [11] H. Li, F.Y. Leong, G. Xu, and et al. Airborne dispersion of droplets dur-
443 ing coughing: a physical model of viral transmission. Sci Rep, 11:4617,
444 2021.
- 445 [12] Leonard F. Pease, Na Wang, Gourihar R. Kulkarni, Julia E. Fla-
446 herty, and Carolyn A. Burns. A missing layer in covid-19 studies:

- 447 Transmission of enveloped viruses in mucus-rich droplets. International
448 Communications in Heat and Mass Transfer, 131:105746, 2022.
- 449 [13] E. P. Vejerano and L. C. Marr. Physico-chemical characteristics of evap-
450 orating respiratory fluid droplets. 15(139), 2018.
- 451 [14] Andrea J. French, Alexandra K. Longest, Jin Pan, Peter J. Vikesland,
452 Nisha K. Duggal, Linsey C. Marr, and Seema S. Lakdawala. Environ-
453 mental stability of enveloped viruses is impacted by initial volume and
454 evaporation kinetics of droplets. 14(2), 2023.
- 455 [15] E. Mikhailov, S. Vlasenko, R. Niessner, and U. Pöschl. Interaction
456 of aerosol particles composed of protein and salts with water vapor:
457 hygroscopic growth and microstructural rearrangement. Atmospheric
458 Chemistry and Physics, 4(2):323–350, 2004.
- 459 [16] Wan Yang, Subbiah Elankumaran, and Linsey C. Marr. Relationship
460 between humidity and influenza a viability in droplets and implications
461 for influenza’s seasonality. PLoS One, 2012.
- 462 [17] David Engler Faleiros, Wouter van den Bos, Lorenzo Botto, and Fulvio
463 Scarano. Tu delft covid-app: A tool to democratize cfd simulations for
464 sars-cov-2 infection risk analysis. Science of The Total Environment,
465 826:154143, 2022.
- 466 [18] Simon Coldrick, Adrian Kelsey, Matthew J. Ivings, Timothy G. Foat,
467 Simon T. Parker, Catherine J. Noakes, Allan Bennett, Helen Rickard,
468 and Ginny Moore. Modeling and experimental study of dispersion and
469 deposition of respiratory emissions with implications for disease trans-
470 mission. Indoor Air, 32(2):e13000, 2022.
- 471 [19] W. Chen, L. Liu, J. Hang, and et al. Predominance of inhalation route
472 in short-range transmission of respiratory viruses: Investigation based
473 on computational fluid dynamics. Build. Simul., 16:765–780, 2023.
- 474 [20] Scientific Advisory Group for Emergencies. Transmission of SARS-CoV-
475 2 and Mitigating Measures. Technical Report June, 2020.
- 476 [21] John E. McCarthy, Barry D. Dewitt, Bob A Dumas, and Myles T.
477 McCarthy. Modeling the relative risk of SARS-CoV-2 infection to in-
478 form risk-cost-benefit analyses of activities during the SARS-CoV-2 pan-
479 demic. PLOS ONE, 16(1):e0245381, jan 2021.

- [22] Lidia Morawska, Joseph Allen, William Bahnfleth, Philomena M. Bluysen, Atze Boerstra, Giorgio Buonanno, Junji Cao, Stephanie J. Dancer, Andres Floto, Francesco Franchimon, Trisha Greenhalgh, Charles Haworth, Jaap Hogeling, Christina Isaxon, Jose L. Jimenez, Jarek Kurnitski, Yuguo Li, Marcel Loomans, Guy Marks, Linsey C. Marr, Livio Mazzarella, Arsen Krikor Melikov, Shelly Miller, Donald K. Milton, William Nazaroff, Peter V. Nielsen, Catherine Noakes, Jordan Peccia, Kim Prather, Xavier Querol, Chandra Sekhar, Olli Seppänen, Shin Ichi Tanabe, Julian W. Tang, Raymond Tellier, Kwok Wai Tham, Pawel Wargocki, Aneta Wierzbicka, and Maosheng Yao. A paradigm shift to combat indoor respiratory infection. Science, 372(6543):689–691, 2021.
- [23] Wenzhao Chen, Nan Zhang, Jianjian Wei, Hui-Ling Yen, and Yuguo Li. Short-range airborne route dominates exposure of respiratory infection during close contact. Building and Environment, 176:106859, jun 2020.
- [24] Yash Shah, John W. Kurelek, Sean D. Peterson, and Serhiy Yarusevych. Experimental investigation of indoor aerosol dispersion and accumulation in the context of covid-19: Effects of masks and ventilation. Physics of Fluids, 33(7):073315, 2021.
- [25] JP Duguid. The size and the duration of air-carriage of respiratory droplets and droplet-nuclei. Epidemiol. Infect., 44(6):471–479, 1946.
- [26] C.Y.H. Chao, M.P. Wan, L. Morawska, G.R. Johnson, Z.D. Ristovski, M. Hargreaves, K. Mengersen, S. Corbett, Y. Li, X. Xie, and D. Katoshevski. Characterization of expiration air jets and droplet size distributions immediately at the mouth opening. Journal of Aerosol Science, 40(2):122–133, 2009.
- [27] William C. Hinds. Aerosol Technology: Properties, Behavior, and Measurement of Airborne Particles. Wiley, 1982.
- [28] PA Baron. Description of an aerosol calculator. In Biswas P., Chen D.R., and Hering S., editors, Proceedings of the Seventh International Aerosol Conference, September 10-15, 2006, St. Paul, Minnesota, USA. American Association for Aerosol Research, Mount Laurel, NJ, 2006.
- [29] Andrew Maynard. <https://hiddenworld.andrewmaynard.me/2020/07/17/how-long-do-aerosols-stay-airborne/>, 2020.

- 514 [30] J.A. Lynch, J.S. Bennett, B.W. Jones, and M.H. Hosni. Viral particle
515 dispersion and viability in commercial aircraft cabins. 2018 ASHRAE
516 annual conference Proceedings, 2018.
- 517 [31] J.S. Bennett, S. Mahmoud, W. Dietrich, B. Jones, and M. Hosni. Evalu-
518 ating vacant middle seats and masks as coronavirus exposure reduction
519 strategies in aircraft cabins using particle tracer experiments and com-
520 putational fluid dynamics simulations. 2022.
- 521 [32] M. Zee, A.C. Davis, A.D. Clark, T. Wu, S.P. Jones, L. L. Waite, J.J.
522 Cummins, and N.A. Olson. Computational fluid dynamics modeling of
523 cough transport in an aircraft cabin. Sci Rep, (11), 2021.
- 524 [33] Gholamhossein Bagheri, Birte Thiede, Bardia Hejazi, Oliver Schlenczek,
525 and Eberhard Bodenschatz. An upper bound on one-to-one exposure
526 to infectious human respiratory particles. Proceedings of the National
527 Academy of Sciences, 118(49):e2110117118, 2021.
- 528 [34] Nicholas R. Jones, Zeshan U. Qureshi, Robert J. Temple, Jessica P.J.
529 Larwood, Trisha Greenhalgh, and Lydia Bourouiba. Two metres or one:
530 what is the evidence for physical distancing in covid-19? BMJ (Clinical
531 research ed.), 370:m3223, 2020.

532 The findings and conclusions in this report are those of the authors and
533 do not necessarily represent the official position of the National Institute for
534 Occupational Safety and Health, Centers for Disease Control and Prevention.

List of Figures

Figure 1:
Flowchart illustrating how five published studies (Chen 2020 [23], Duguid 1946 [25], Chao 2009 [26], Shah 2021 [24], Lynch 2018 [30]) are used to form the current model involving distance, particle size (droplets, aerosol) and exposure route (Routes 1 & 2).

Figure 2:

Decrease of risk, as virion exposure, with distance from an infectious person. The key finding is that for short distances both Routes 1 and 2 are important sources of exposure (estimated in two different ways, shown by blue and orange curves), because the decay is steeper than for the longrange models. For these longer distances the primary source of exposure is aerosols and Route 2 (estimated in two different ways, shown by gray and yellow curves). The decrease measured in 737 (first figure) and 767 (second figure) mock-up tracer experiments is normalized or "anchored" to intersect the speaking data at 2m from Chao (gray) and Duguid (yellow). The anchor values from Table 3 are plotted on the log base 10 scale. The superposed risk is the sum of the droplet and aerosol exposure risk. We plot the sum of the maximum and the minimum of the two estimates and note that these are larger than the trend predicted by the longrange data.

List of Tables

Table 1: Volume of various droplet sizes from Chao (2009) [26] (C) and Duguid (1946) [25] (D).

Table 2: Adapted from Shah (2021) [24]. First column indicates whether the exhaling mannikin is wearing a mask. Second column is the number of air changes per hour. Third column is the percentage of exhaled particles that arrive at the detector every hour. Fourth column is the particle loss rate parameter. Fifth column is the steady state or saturation concentration as a percentage of the emission rate.

Table 3: Steady-state aerosol intake in pL for every 1 μ L emitted, at a 2 m distance from the source (from Chao (2009) [26], Duguid (1946) [25], and Shah (2021) [24]).